

# DNA Bending Is a Determinant of Calicheamicin Target Recognition<sup>†</sup>

Aaron A. Salzberg<sup>‡</sup> and Peter C. Dedon\*

Division of Bioengineering and Environmental Health, 56-787, Massachusetts Institute of Technology, Cambridge, Massachusetts 02139

Received September 24, 1999; Revised Manuscript Received March 28, 2000

**ABSTRACT:** Calicheamicin is a hydrophobic enediyne antibiotic that binds noncovalently to DNA and causes sequence-selective oxidation of deoxyribose. While the drug makes several base contacts along the minor groove, the diversity of binding-site sequences and the effects of DNA conformation on calicheamicin-induced DNA cleavage suggest that sequence recognition per se is not the primary determinant of target selection. We now present evidence that calicheamicin bends its DNA targets. Using a gel mobility assay, we observed that polymers of oligonucleotide constructs containing AGGA and ACAA binding sites for calicheamicin did not possess intrinsic curvature. Binding of calicheamicin  $\epsilon$ , the aromatized form of the parent calicheamicin  $\gamma_1^I$ , to oligonucleotide constructs containing binding sites in phase with the helical repeat caused a shift to smaller circle sizes in T4 ligase-mediated circle formation assays, with a much smaller shift observed with constructs containing out-of-phase binding sites. It was also observed that binding of calicheamicin  $\epsilon$  to a 273 bp construct with phased binding sites caused an increase in the molar cyclization factor,  $J$ , from  $8 \times 10^{-8}$  to  $9 \times 10^{-6}$  M. These results are consistent with DNA bending as part of an induced-fit mechanism of DNA target recognition and with the hypothesis that the preferred targets of calicheamicin, the 3' ends of oligopurine tracts, are characterized by unique conformational properties.

The sequence selectivities of several genotoxic chemicals that bind covalently to DNA have been shown to depend, at least in part, on the ability of specific DNA sequences to undergo conformational changes (e.g., refs 3–5). However, the role of DNA structure and dynamics in the targeting of small, noncovalently binding chemicals remains enigmatic, particularly for hydrophobic molecules that do not bind DNA with high enough affinity to use standard electrophoretic techniques for investigating DNA topology. We have overcome this problem and now present evidence that DNA bending plays a role in the selection of DNA targets by calicheamicin  $\gamma_1^I$ .

Calicheamicin  $\gamma_1^I$  is a member of the enediyne class of antitumor antibiotics (Figure 1; reviewed in refs 4–7). This extremely potent cytotoxin damages DNA by binding noncovalently in the minor groove and rearranging to a benzenoid diradical intermediate that abstracts hydrogen atoms from deoxyribose, which leads to high levels of double-stranded DNA lesions (6–9). While this mechanism is well established, the process by which enediynes select their DNA targets is poorly understood.

Calicheamicin target selection was initially observed to involve tetrapurine sequences such as AGGA and AAAA (10–12). However, recent studies have revealed that calicheamicin generally recognizes the 3'-end of purine tracts (13, 14). The drug binds the DNA in the minor groove with

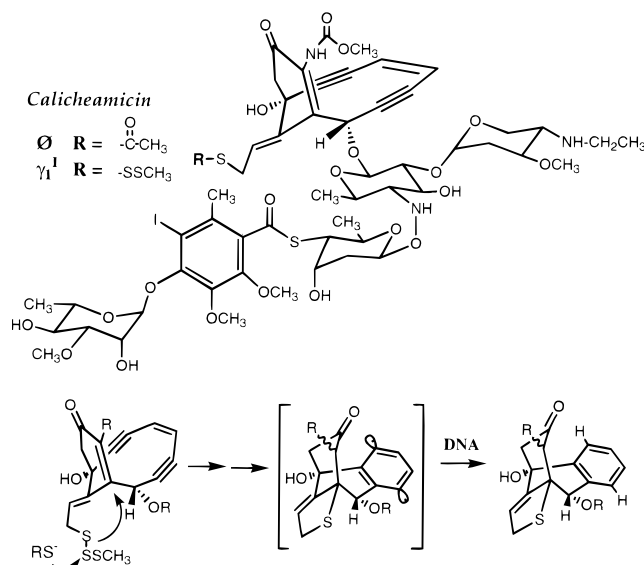


FIGURE 1: Structures of calicheamicins  $\gamma_1^I$ ,  $\epsilon$ , and  $\phi$ .

the aglycon positioned at the 3' end of the purine tract and the carbohydrate tail extending in the 5' direction (15–19). While ionic interactions do not appear to play an important role in binding of the drug to DNA (20), NMR studies have revealed that calicheamicin forms minor-groove hydrogen bonds with bases and phosphate oxygens (16, 17, 19). van der Waals contacts also occur between the pyrimidine bases of the target sequence and the oligosaccharide tail, which is responsible for calicheamicin's sequence selectivity (21, 22). However, it is unlikely that these interactions fully account for target recognition since the drug binds to a wide variety of base sequences (10–14).

<sup>†</sup> This work was supported by NIH Grants CA64524 and CA72936 (P.C.D.) and NIEHS Training Grant ES07020 (A.A.S.).

\* To whom correspondence should be addressed: phone 617-253-8017; fax 617-258-0225; e-mail pcdedon@mit.edu.

<sup>‡</sup> Present address: U.S. Department of State, OES/PCI Room 7821, 2201 C Street N.W., Washington, DC 20520.

Hydrophobic interactions also appear to play an important role in calicheamicin binding to DNA (23). Since homopurine sequences are more hydrated than mixed-sequence DNA (24), entropic effects may make substantial contributions to the thermodynamics of binding to oligopurine tracts. This does not, however, explain why most of the calicheamicin-induced DNA damage occurs at the 3' ends of purine tracts (13, 14).

Several observations suggest a direct role for DNA conformation in the target recognition process of calicheamicin. First, it has been observed that calicheamicin-induced DNA damage is affected by the sequence context of the binding site (e.g., damage at AGGGTC is 40% greater than at AGGGTG; 10, 13, 20). In other words, changes outside the four base pairs making contact with the drug can influence binding. Second, it has been observed that incorporation of DNA into a model nucleosome enhances calicheamicin-induced DNA damage at one site (13, 25). Of several mechanisms that could account for this phenomenon, it is possible that a change in the topology of this calicheamicin binding site caused an increase in its reactivity. A recent study by Sissi et al. (26) lends support to this model. They observed that transcription factor-induced changes in DNA conformation affect calicheamicin binding and damage, with protein-mediated narrowing of the minor groove causing a reduction in drug-induced cleavage (26). Both of these observations are consistent with shape recognition as a mechanism of calicheamicin target selection. Finally, results from circular dichroism (27), DNA sedimentation (28), and NMR (16, 17, 19) studies are consistent with drug-induced changes in DNA conformation, while protein binding studies suggest that DNA flexibility contributes to drug binding (26). Together, these data highlight the importance of DNA conformation in target recognition by calicheamicin and suggest that an induced-fit mechanism plays an important role in determining where calicheamicin binds.

To test this hypothesis, we have investigated the characteristics of calicheamicin binding sites with a strategy generally applicable to other noncovalently binding, DNA-modifying chemicals regardless of their hydrophobicity. Using gel mobility assays, we first determined whether an element of intrinsic DNA curvature was common to non-A-tract drug binding sites. Then, using two different DNA cyclization techniques, we established the effects of calicheamicin binding on DNA structure.

## MATERIALS AND METHODS

**Reagents and DNA Substrates.** Calicheamicins  $\gamma_1^I$  and  $\epsilon$  were provided by Dr. George Ellestad (Wyeth Ayerst Research, Pearl River, NY); calicheamicin  $\phi$  was provided by Professor K. C. Nicolaou (Scripps Research Institute). All enzymes were obtained from New England Biolabs. Deoxyoligonucleotides (21 nt;<sup>1</sup> Figure 2) were either synthesized (Applied Biosystems; Biogenex reagents) or purchased (Oligos Etc.; Portland, OR) and purified as described elsewhere (29).

Cloned polymers of the calicheamicin binding-site constructs (Figure 2) were prepared by annealing complementary oligonucleotides to form duplex monomers that were then

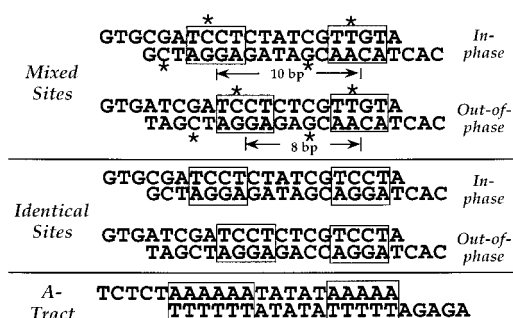


FIGURE 2: Calicheamicin binding site constructs. Boxes denote calicheamicin binding sites or curved DNA sequences (A-tracts). Asterisks indicate sites of calicheamicin  $\gamma_1^I$  cleavage.

ligated to produce a population of multimers. The polymers were ligated into a modified pUC19 cloning vector (pAS1) containing a single *SapI* recognition site with GTG and CAC ends (A. Salzberg and P. Dedon, unpublished results). Clones containing specific multimers were isolated from a non-methylating strain of *Escherichia coli* (GM2163) and characterized for sequence and size. Cloned restriction fragments were purified by polyacrylamide gel electrophoresis (PAGE; 26).

**Characterization of Calicheamicin Binding Sites.** Plasmids containing polymers of the binding-site constructs were digested with *EcoRI* and 5'-<sup>32</sup>P-end-labeled by standard techniques (30). Labeled DNA was digested with *HindIII* and the polymer-containing restriction fragment was purified by nondenaturing polyacrylamide gel electrophoresis (30). Damage reactions consisted of labeled DNA (~50 000 cpm), 30  $\mu$ g/mL sheared and exonuclease-trimmed calf thymus DNA, 10 mM glutathione, 50 mM HEPES, and 1 mM EDTA (pH 7). The reaction was initiated by adding calicheamicin  $\gamma_1^I$  (30 nM; final 1% methanol). After 1 h at 0 °C, the DNA was ethanol precipitated and resolved on an 8% sequencing gel.

**Assessment of Calicheamicin Binding-Site Interactions.** Cloned plasmids were digested with *XbaI* and 5'-<sup>32</sup>P-end-labeled (30). Following digestion with *EcoRI*, the labeled fragment was purified as described above. Damage reactions consisted of labeled DNA (~30 000 cpm), 30  $\mu$ g/mL calf thymus DNA, 10 mM glutathione, 10 mM HEPES, and 1 mM EDTA (pH 7). The reaction was initiated by adding calicheamicin  $\phi$  and then glutathione to the following final concentrations, respectively: 0.1  $\mu$ M and 10 mM; 1  $\mu$ M and 10 mM; 10  $\mu$ M and 1 mM; and 100  $\mu$ M and 0 mM. After  $\geq 1$  h at 37 °C, the DNA was ethanol precipitated and resolved on a 6% sequencing gel.

**Gel Mobility Analysis of Binding Site Constructs.** Annealed and 5'-<sup>32</sup>P-end-labeled 21 bp binding site constructs (7.5  $\mu$ M) or *BamHI* linkers (New England Biolabs) were treated with T4 DNA ligase (8 units/mL) overnight at 16 °C in 50 mM Tris-HCl (pH 7.8), 10 mM MgCl<sub>2</sub>, 10 mM dithiothreitol, 1 mM ATP, and 50  $\mu$ g/mL bovine serum albumin. The reaction was stopped with EDTA and the DNA was purified by phenol/chloroform extraction and ethanol precipitation. Ligation products were then resolved on a nondenaturing 8% polyacrylamide gel. Following phosphorimager analysis (Molecular Dynamics), the relative mobility of individual polymers was determined by dividing the apparent length, based on *BamHI* linker migration, by the actual length. *BamHI* linker polymers have been shown to migrate with

<sup>1</sup> Abbreviations: bp, base pair; nt, nucleotide.

normal mobility (31, 32) and we confirmed this by comparison to *Msp*I-digested pBR322 (data not shown).

**T4 Ligase Circle Formation Assays.** Annealed 21 bp DNA constructs (1.4  $\mu$ g) were 5'-<sup>32</sup>P-end-labeled (30) and then quantified by UV spectroscopy. DNA (120 ng) was ligated at 16 °C overnight with 400 units of T4 DNA ligase in a total volume of 50  $\mu$ L containing 50 mM Tris-HCl (pH 7.5), 10 mM MgCl<sub>2</sub>, 10 mM dithiothreitol, 1 mM ATP, 25  $\mu$ g/mL bovine serum albumin, and varying concentrations of calicheamicin  $\epsilon$ . The DNA was purified by phenol/chloroform extraction and ethanol precipitation.

Visualization of circular DNA products by one-dimensional polyacrylamide gel electrophoresis was accomplished by removing linear DNA polymers with Bal 31 exonuclease as described elsewhere (29). The identity of bands remaining after exonuclease digestion of linear polymers was established by eluting DNA bands from a 6% nondenaturing polyacrylamide gel, denaturing the DNA by heating at 90 °C for 5 min, and then resolving the DNA on an 8% denaturing polyacrylamide gel containing 6 M urea.  $\gamma$ -Radiation-induced nicking of the circles produced linearized strands that migrated normally and intact circular strands displaying retarded migration (33). Gels containing Bal 31-digested DNA were dried and subjected to phosphorimager analysis. The quantity of radioactivity in a band representing a DNA circle was normalized according to circle size and the percentage of each circle was then expressed as the proportion of total radioactivity of all the circles measured. The arithmetic mean was computed from the distribution of circles formed. In all cases, nonligatable substrate DNA accounted for less than 5% of the total of radioactively labeled species (i.e., circles and linear molecules). Furthermore, incomplete ligation leading to nicked polymers appeared to be minimal as judged by (1) the presence of less than 10% single-stranded linear DNA molecules in sequencing gels containing circular species isolated from nondenaturing gels and (2) similar amounts of radioactivity (phosphorimager analysis) in linear polymer bands in sequencing and nondenaturing gels (data not shown).

**DNA Cyclization Kinetics.** A 5'-<sup>32</sup>P-end-labeled 273 bp or 63 bp polymer of the in-phase mixed-site construct was combined with unlabeled polymer at a ratio of less than 1:20 (34) and the DNA ligated at 20 °C in a reaction containing 65 nM DNA polymer, 50 mM Tris-HCl (pH 7.8), 10 mM MgCl<sub>2</sub>, 10 mM dithiothreitol, 1 mM ATP, 50  $\mu$ g/mL bovine serum albumin, 1.3% methanol, 0–1 mM calicheamicin  $\epsilon$ , and 0.01 unit/mL T4 DNA ligase. Aliquots (10  $\mu$ L) were removed at various times and the reaction was quenched by adding 5  $\mu$ L of 100 mM EDTA (pH 8), 0.04% bromophenol blue, and 5% glycerol and heating at 65 °C for 10 min. Cooled samples were loaded onto a 4% polyacrylamide gel. The quantity of radioactivity in each band was determined by phosphorimager analysis and the reaction rates were determined as described elsewhere (35, 36). In control experiments with extended incubation times, nonligatable monomer species accounted for less than 5% of the total of radioactively labeled species.

**Hazardous Procedures.** Calicheamicin is an extremely toxic DNA-damaging agent and great care must be exercised in its handling.

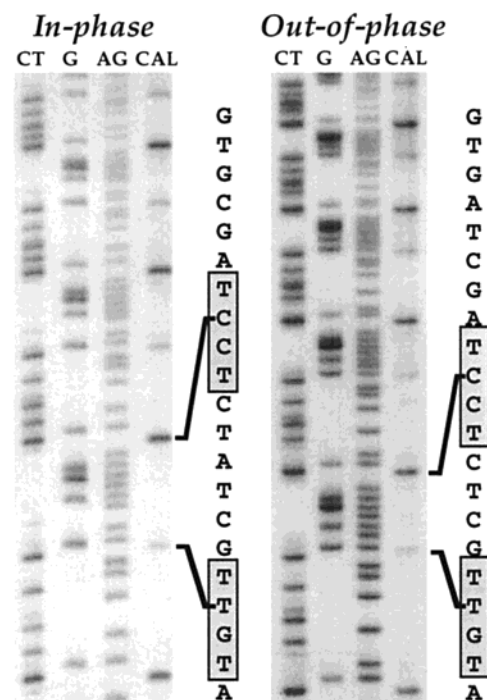


FIGURE 3: Calicheamicin  $\gamma_1$ -induced DNA damage in the binding-site constructs. Labeled polymers of the mixed-site constructs were treated with 30 nM calicheamicin  $\gamma_1$  and resolved on a sequencing gel (CAL) as described in Materials and Methods. The location of damage sites is indicated in the diagrams to the right of each gel. Lanes containing untreated DNA showed no detectable damage (data not shown). Lanes marked CT, G, and AG represent chemical sequencing standards (30).

## RESULTS

**Design of Calicheamicin Binding Site Constructs.** A series of 21 bp duplex oligonucleotides was designed to investigate both the structural features of calicheamicin binding sites and the effects of drug binding on DNA conformation. As shown in Figure 2, the 21 bp constructs contained calicheamicin binding sequences aligned in various relationships to the helical repeat of B-DNA. One set of constructs contained AGGA•TCCT and ACAA•TTGT binding sites (6, 11); the other set contained two AGGA•TCCT binding sites. In all cases, the purine-rich sequences were on the same strand so that the drug bound in the same orientation at each site. The in-phase constructs had binding sites positioned 10 bp apart to ensure that multimers had binding sites spaced—on average—in phase with the 10.5 bp helical repeat of B-DNA. Therefore, any localized bending or anisotropic flexibility would add constructively and lead to macroscopic curvature. The two out-of-phase monomers contain the same binding sequences spaced 8 bp apart. Together with the in-phase DNA molecules, these constructs allow us to distinguish between twist- and bend-induced changes in the rate of cyclization. The 3 bp complementary ends (*Sap*I cleavage sites) were necessary to avoid creation of additional drug binding sites while allowing cloning of the polymers. The final 21 bp monomer has two phased A-tracts and has been shown to produce curved multimers (33).

To ensure that the DNA constructs possessed the predicted binding sites, multimers of each monomer were damaged with calicheamicin  $\gamma_1$  and the cleavage products were analyzed on sequencing gels. As shown in Figure 3, the mixed-site polymers were damaged only at the expected sites.



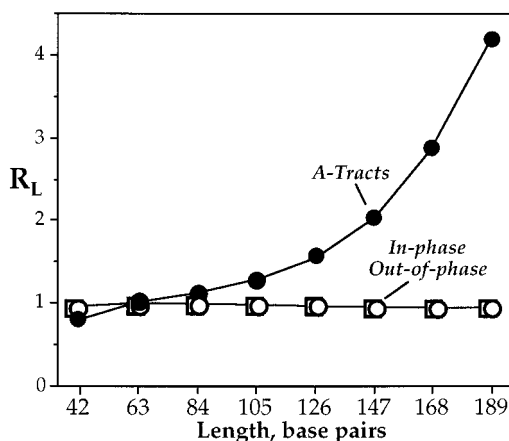


FIGURE 4: Relative mobility of polymers of calicheamicin binding site constructs plotted as a function of DNA size. Labeled duplex oligonucleotide constructs were polymerized with T4 DNA ligase and the DNA polymers were resolved on a 10% nondenaturing polyacrylamide gel as described under Materials and Methods. The mobility of the construct polymers relative to polymerized *Bam*HI linkers,  $R_L$ , was determined by phosphorimager analysis.

Consistent with previous studies, damage at the AGGA site occurred more frequently than at the ACAA site (11, 37). The observation that the ratio of damage between the two sites is nearly equal for both polymers (3.8 and 3.6 for the in-phase and out-of-phase constructs, respectively) suggests that shortening the distance between the two binding sites does not affect drug binding at either site. This is supported by hydroxyl radical footprinting studies that revealed equivalent binding of calicheamicin  $\epsilon$ , under saturating conditions, to sites separated by 8 bp (37).

To verify that that drug binding to one site did not interfere with binding to an adjacent site, we performed a second series of damage studies with calicheamicin  $\phi$ , a calicheamicin  $\gamma_1^I$  analogue with a thioacetate trigger instead of a methyltrisulfide (Figure 1; 38). With calicheamicin  $\phi$ , it is possible to measure drug-induced DNA damage over a broad range of drug concentrations by titrating the amount of glutathione activator so that similar levels of DNA damage are produced. In the range of drug concentrations tested (1–100  $\mu$ M), the ratio of calicheamicin  $\phi$ -induced DNA damage at neighboring binding sites was the same in both the in-phase and out-of-phase constructs (data not shown). These results indicate that, even at high concentrations, calicheamicin binds without detectable interaction between the binding sites in the in-phase and out-of-phase constructs. This comparison of calicheamicins  $\phi$ ,  $\epsilon$ , and  $\gamma_1^I$  is justified by the fact that all three molecules bind to DNA by identical mechanisms, as revealed in NMR studies (17, 39), and with the same relative affinity for the different sites (e.g., AGGA versus ACAA; present data and ref 36).

**Relative Electrophoretic Mobility of Calicheamicin Binding Constructs.** To assess the intrinsic curvature of the calicheamicin binding sites, we examined the migration of polymers of the mixed-site constructs by gel electrophoresis. These studies are premised upon the anomalously slow migration of curved DNA on polyacrylamide gels (39–42). In Figure 4, the relative mobilities of polymers from the self-ligation of the mixed-site constructs are compared with the curved A-tract DNA. None of the binding site constructs exhibited significant migration anomalies. As a result, we can conclude that the two calicheamicin binding sites tested

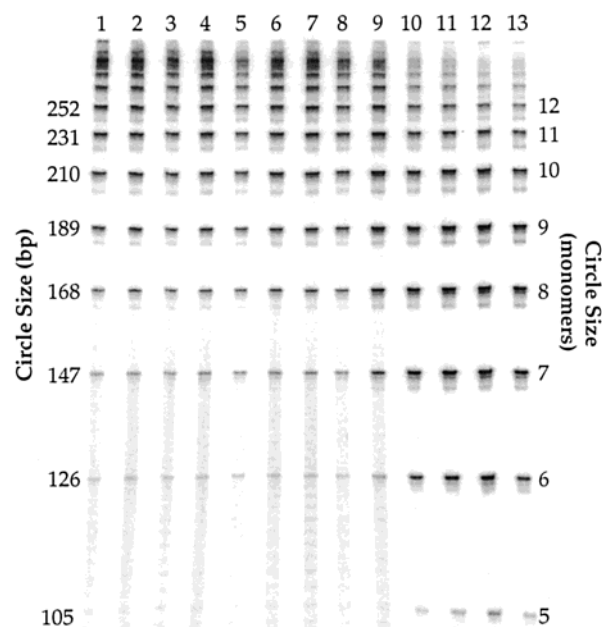


FIGURE 5: Effect of calicheamicin  $\epsilon$  on circle size in the ligase-mediated circle closure assay. Labeled duplex oligonucleotide constructs were polymerized with T4 DNA ligase in the presence of varying concentrations of calicheamicin  $\epsilon$ , linear DNA polymers were removed with Bal 31, and the remaining DNA polymers were resolved on a 10% nondenaturing polyacrylamide gels. Calicheamicin  $\epsilon$  concentrations in lanes 1–13 were 0, 0.02, 0.08, 0.3, 0.6, 1.25, 1.9, 2.5, 5, 10, 20, 40, and 400  $\mu$ M.

do not possess significant curvature and that sequence-dependent curvature is not the sole mediator of calicheamicin binding.

**Effect of Calicheamicin  $\epsilon$  on the Ligase-Catalyzed DNA Circularization Assay.** As suggested earlier, DNA binding by calicheamicin may be facilitated by the deformation of specific sequences to accommodate binding of the drug. If true, the drug–DNA complex should reflect these changes. To assess the effect of calicheamicin binding on DNA structure, we measured the ability of a DNA molecule—with phased calicheamicin binding sites—to cyclize as increasing amounts of drug were bound. These experiments rely on the fact that curved or bent DNA sequences, when repeated in phase with the DNA helical repeat, cause the two ends of the DNA molecule to be near each other more frequently than in “straight” DNA (33, 34, 41, 43). Empirically, this curvature can be measured by covalently “trapping” the ends of a DNA molecule with T4 DNA ligase to form circles. The distribution of different sized circles (represented by the mean) then reflects changes in the average probability of cyclization for a specific family of DNA polymers (29).

Using one-dimensional gel electrophoresis, we examined the circular products formed from the self-ligation of the in-phase, mixed-site construct (29). The inactivated form of calicheamicin  $\gamma_1^I$ , calicheamicin  $\epsilon$  (Figure 1), was used since the presence of dithiothreitol in the ligase stock solution can activate the native drug to produce double-strand DNA breaks. Previous studies have shown that both forms of calicheamicin bind to the same DNA sequences (11, 37) by identical mechanisms (19), although the  $\epsilon$  form binds with lower affinity (27).

As shown in Figure 5, increasing concentrations of calicheamicin  $\epsilon$  result in the formation of smaller circles.

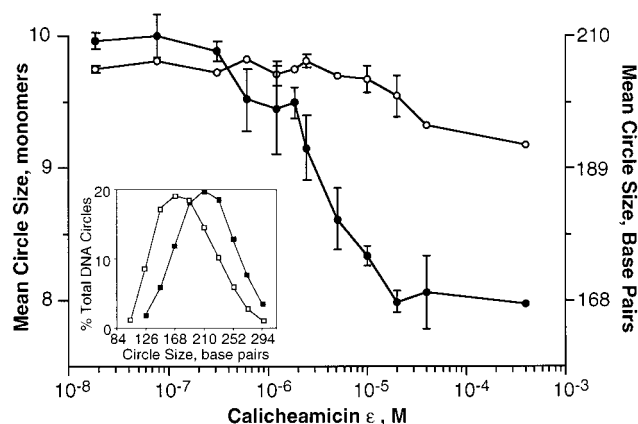


FIGURE 6: Mean circle size plotted as a function of calicheamicin  $\epsilon$  concentration. Mean circle size was determined as described under Materials and Methods. Solid circles correspond to the in-phase, mixed-site construct and open circles correspond to the out-of-phase, mixed-site construct. Error bars represent the standard error for experiments performed in triplicate or deviation about the mean for duplicate results. The inset shows the variation in circle size following T4 ligase-mediated polymerization of the in-phase construct in the presence ( $\square$ ) and absence ( $\blacksquare$ ) of 5  $\mu$ M calicheamicin  $\epsilon$ .

This change is shown graphically in Figure 6, where it can be seen that drug binding lowers the mean of the circle size distributions from a  $\sim$ 10-mer to an  $\sim$ 8-mer (210 to 168 bp). The sigmoidal shape of the graph likely reflects both the binding isotherm of calicheamicin and the biophysical limits of the assay. Similar results were obtained with the in-phase, identical-site construct (data not shown).

Since the ability of a molecule to cyclize is dependent upon both the relative proximity and alignment of its ends, three factors could account for these results: (1) calicheamicin increases the probability of cyclization regardless of the DNA sequence; (2) binding of calicheamicin introduces phased bends into the polymer, bringing the ends closer together and increasing the probability of cyclization; and/or (3) drug binding alters the helical rotation of the polymer such that the ends are more favorably aligned for cyclization. To rule out both sequence-independent effects and the contribution of helical rotation, we repeated the DNA cyclization experiment with the out-of-phase, mixed-site DNA construct. The results are shown in Figure 6. While there is a slight shift to smaller circle sizes in the presence of similar concentrations of calicheamicin  $\epsilon$ , drug binding to the out-of-phase construct did not produce the large shift seen with the in-phase construct. Similar data were obtained with identical-site monomer (data not shown). This observation ruled out options 1 and 3 since, for either to be true, the out-of-phase constructs would have to exhibit the same behavior as the in-phase constructs (Figure 6). In the latter case, this is because localized twisting of the helical axis affects the alignment of the ends regardless of where in the strand it occurs.

The small shift in the mean circle size for the out-of-phase construct may be the result of different binding affinities between the two sites, incomplete cancellation of the bend components, or some degree of drug-induced twist. However, since a significant calicheamicin-induced reduction in circle size was apparent only with the in-phase constructs, we conclude that a major portion of the change observed in the cyclization properties must be a response to bending.

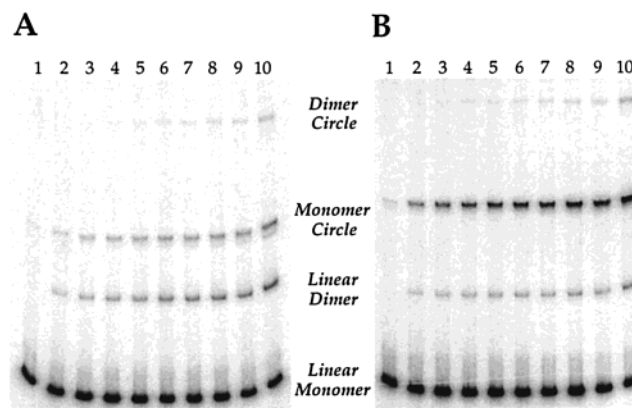


FIGURE 7: Effect of calicheamicin  $\epsilon$  on the kinetics of DNA cyclization. A 273 bp polymer of the in-phase, mixed-site construct was reacted with DNA ligase in the absence (A) or presence (B) of 3  $\mu$ M calicheamicin  $\epsilon$ . The products were resolved on a 4% nondenaturing polyacrylamide gel as described under Materials and Methods. Lanes 1–10 represent time points of 0, 0.5, 1, 1.5, 2, 2.5, 3, 4, 5, and 10 min.

Consistency in the quantity of both circular and linear polymerization products over the full range of calicheamicin  $\epsilon$  concentrations suggest that calicheamicin  $\epsilon$  had no effect on ligase activity (data not shown).

**Effect of Calicheamicin  $\epsilon$  on the Rate of Cyclization.** To rigorously quantify the effects of calicheamicin binding on DNA structure, we used a more sensitive version of the DNA cyclization assay (1, 34, 35, 44, 45). Rather than examining the cyclization of a family of polymers, we ligated a single 273 bp DNA polymer (13 repeats of the in-phase, mixed-site construct) under conditions that produced both circles and dimers. By measuring the amount of individual reaction products formed over time, the rate constants for the competing cyclization ( $k_1$ ) and bimolecular association ( $k_2$ ) reactions were estimated. Under the proper conditions (35), which are satisfied in the present experiments,

$$f(k_1, k_2) \approx f(K_c, K_a) = J$$

where  $K_c$  and  $K_a$  are the equilibrium constants for cyclization and bimolecular association, respectively, and  $J$  is the ring closure probability (Jacobson–Stockmayer factor in units of molar concentration). Changes in the probability of cyclization reflect bending and twisting of the DNA helix.

Figure 7 shows examples of the time-dependent ligation products of the 273 bp polymer at two different calicheamicin  $\epsilon$  concentrations. The individual rate constants were estimated at several drug concentrations (0.1–10  $\mu$ M) and the probability of cyclization was determined (Figure 8); drug concentrations of 31 and 100  $\mu$ M were not used in the kinetics calculations since they produced only circular products. In the absence of calicheamicin  $\epsilon$ , the probability of cyclization is  $8 \times 10^{-8}$  M (Figure 8B). This value is similar to that obtained by Shore and Baldwin for a 250 bp DNA fragment with a four nucleotide AATT overhang<sup>2</sup> (1), but it is somewhat higher than other similarly sized DNA fragments (1, 43). On the other hand, our value of  $8 \times 10^{-8}$

<sup>2</sup> The base pairing energetics of the AATT overhang in the fragments used by Shore and Baldwin (1) and the GTG overhang used in our studies are estimated to be quite similar at  $\Delta G \sim -0.8$  and  $-0.9$  kcal/mol, respectively (2).

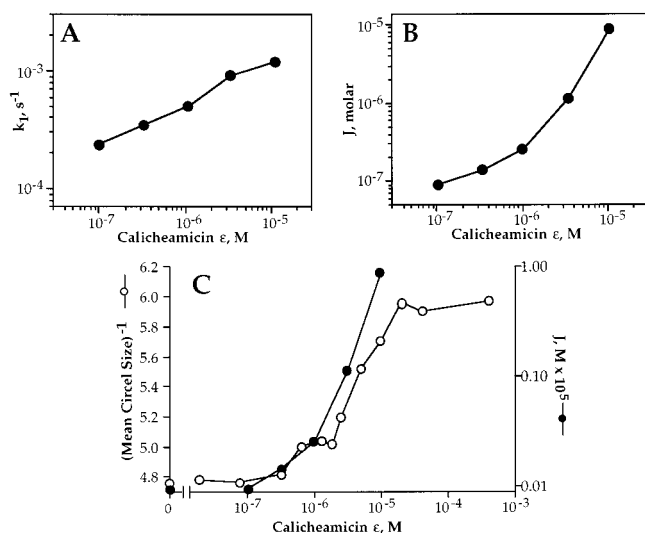


FIGURE 8: DNA cyclization kinetics for the 273 bp polymer as a function of calicheamicin  $\epsilon$  concentration. (A) Rate of cyclization,  $k_1$  (s<sup>-1</sup>). (B) Probability of cyclization,  $J$  (M). Rates were determined from data partially represented in Figure 7 as described under Materials and Methods. (C) Comparison of  $J$  (●) and mean circle size (○) as a function of calicheamicin  $\epsilon$  concentration.

$M$  is less than that expected for an intrinsically curved polymer consisting of phased A-tracts (35, 46). As revealed in the analyses performed by Hagerman and Ramadevi (44) and Shore and Baldwin (1),  $J$  is heavily dependent on the torsional alignment of the ends of a DNA molecule and thus on the sequence-dependent helical repeat of the DNA fragment. The relatively large  $J$  value for the 273 bp fragment used in the present studies may thus reflect an optimal alignment of the ends of the fragment; phased curvature has been ruled out in the gel mobility studies.

The most important result of this experiment is the smooth increase in  $J$  as a function of drug concentration over the range of 0.5–35% binding site occupancy (based on an association constant of  $6 \times 10^4$  M<sup>-1</sup>; see refs 26 and 46). The 31 and 100  $\mu$ M calicheamicin  $\epsilon$  concentrations—that caused only circle formation—are calculated to produce 62% and 85% occupancy, respectively. The increase in  $J$  as a function of calicheamicin  $\epsilon$  concentration is consistent with drug-induced DNA bending. Drug-induced twisting cannot fully explain the results since it is expected that the 273 bp binding-site construct would display a similar sensitivity to twist-mediated end-alignment effects as the 237–254 bp fragments employed by Shore and Baldwin (1). We would therefore expect that progressive changes in twist caused by drug binding would produce an oscillatory behavior in the  $J$  values. The smooth curve shown in Figure 8 suggests that intermediate drug concentrations will not produce wide swings in  $J$ .

## DISCUSSION

Calicheamicin is a potent antitumor antibiotic that causes sequence-selective oxidation of the deoxyribose of DNA (6, 8, 9, 48). Although the drug makes several base-specific contacts along the minor groove, the broad range of sequences bound (10–14), the sensitivity of calicheamicin-induced DNA damage to neighboring sequences (10, 27), and the modulation of drug binding by protein-induced alterations of the target site (13, 25, 26, 49) all suggest that

sequence recognition per se is not the primary determinant of target selection. These observations imply that DNA structure and dynamics mediate, at least in part, the binding of calicheamicin. We now provide evidence that this is indeed the case and that calicheamicin bends DNA.

We have shown that two different high-affinity calicheamicin binding sites are not inherently curved and that calicheamicin binding to these target sequences alters the direction of the helix axis. The results of our studies do not permit a quantitative assessment of the magnitude or directionality of the drug-induced DNA bend. As illustrated by Hagerman and Ramadevi (44), the estimation of bend angle from the most prevalent circle size in oligonucleotide polymerization studies can lead to significant error. However, it is clear from Figure 8C that increasing the calicheamicin  $\epsilon$  concentration over the range of 10<sup>-7</sup>–10<sup>-5</sup> M produces parallel changes in  $J$  and mean circle size (i.e., increase in  $J$  and decrease in circle size). The similar behaviors of the two systems suggests that there is a quantitative relationship between the molar cyclization factor and mean circle size, a relationship that warrants further investigation.

The observed deformation of DNA structure upon binding of calicheamicin provides direct physical evidence for a model in which the drug alters local DNA conformation to optimize a constellation of drug–DNA bonding interactions. Recognition of binding sequences by calicheamicin involves hydrogen bonds with several bases and phosphate oxygens in the minor groove (16, 17, 19) as well as van der Waals contacts between the oligosaccharide tail and the pyrimidine bases of the purine tract (21, 22). Hydrophobic interactions also appear to play an important role in calicheamicin binding to DNA (23), possibly by virtue of the increase in entropy accompanying expulsion of water molecules from homopurine sequences, which are more hydrated than mixed-sequence DNA (24).

Our observation of DNA bending by calicheamicin is consistent with a deformation of the DNA helix that accompanies or exists prior to the formation of these bonds. On the basis of NMR data, Kahne and co-workers (50) have proposed that the relatively rigid carbohydrate tail exerts steric pressure on the pyrimidine strand, which leads to widening of the minor groove at the binding site (15, 16). Though our data do not permit determination of the direction of DNA bending, minor-groove widening suggests bending toward the major groove. This would be consistent with the observed reduction of calicheamicin damage occurring as a result of protein-induced bending and subsequent narrowing of the minor groove (26).

Drug-induced deformation of the helix may thus be a simple consequence of optimizing the various bonding interactions at the target site. Since DNA deformation must occur prior to or in concert with drug binding, it would be argued that calicheamicin binding sites are not necessarily curved, such as the AAAA·TTTT damage site, but are instead DNA sequences that can be bent or “trapped” in a conformation that fosters drug binding. The preferred targets of calicheamicin binding, the 3′ ends of oligopurine tracts (13, 14), may thus be characterized by unique properties of conformation or dynamics. This is consistent with observations of A- and G-tract DNA that suggest the existence of a structural discontinuity at the 3′ end of the homopurine sequences (51, 52). However, it is important to note that our



studies do not permit the assessment of DNA flexibility. This would require a systematic determination of persistence lengths, helical repeats, and torsional elastic constants for calicheamicin binding site constructs, which is beyond the scope of the present studies.

Although it is important to the recognition process, we are not proposing that DNA deformation is the solitary determinant of calicheamicin binding. In fact, it is clear that calicheamicin target selection is a complex process involving several interactions that are optimized by the conformational alterations of specific DNA sequences. In cases where the DNA is bent, such as A<sub>4</sub> sequences, the energetic cost of drug binding is reduced by external forces that either bend or move the DNA. However, for those DNA targets considered "straight," a balance must be achieved between the intrinsic resistance of DNA to movement and those forces (e.g., electrostatic and hydrophobic) involved in the binding of calicheamicin to DNA. In addition, since the binding characteristics of individual sequences are heterogeneous, we should expect not one but several optimal binding scenarios, each unique to a particular sequence. As a result, the amount of bending induced need not be uniform across all calicheamicin binding sites.

## ACKNOWLEDGMENT

We thank K. C. Nicolaou and George Ellestad for providing calicheamicin  $\phi$  and calicheamicins  $\gamma_1^I$  and  $\epsilon$ , respectively. We also gratefully acknowledge Punam Mathur for performing the calicheamicin damage studies and William LaMarr, Daniel Lopez-Larazza, Kathleen Vokes, and Jionggu Wu for their technical assistance.

## REFERENCES

- Shore, D., and Baldwin, R. L. (1983) Energetics of DNA twisting. I. Relation between twist and cyclization probability. *J. Mol. Biol.* **170**, 957–981.
- SantaLucia, J., Jr. (1998) A unified view of polymer, dumbbell, and oligonucleotide DNA nearest-neighbor thermodynamics. *Proc. Natl. Acad. Sci. U.S.A.* **95**, 1460–1465.
- Kizo, R., Draves, P. H., and Hurley, L. H. (1993) Correlation of DNA sequence specificity of anthramycin and tomaymycin with reaction kinetics and bending of DNA. *Biochemistry* **32**, 8712–8722.
- Sun, D., Lin, C. H., and Hurley, L. H. (1993) A-tract and (+)-CC-1065-induced DNA bending of DNA. Comparison of structural features using nondenaturing gel analysis, hydroxyl-radical footprinting, and high-field NMR. *Biochemistry* **32**, 4487–4495.
- Hurley, L., Lee, C. S., McGovern, P., Warpehoski, M., Mitchell, M., Kelly, R., and Aristoff, P. (1988) Molecular basis for sequence-specific DNA alkylation by CC-1065. *Biochemistry* **27**, 3886–3892.
- Lee, M. D., Ellestad, G. A., and Borders, D. B. (1991) Calicheamicins: Discovery, structure, chemistry, and interaction with DNA. *Acc. Chem. Res.* **24**, 235–243.
- Nicolaou, K. C., Smith, A. L., and Yue, E. W. (1993) Chemistry and biology of natural and designed enediynes. *Proc. Natl. Acad. Sci. U.S.A.* **90**, 5881–5888.
- Doyle, T. W., and Borders, D. B. (1995) Eneidyne antitumor antibiotics, in *Eneidyne Antibiotics as Antitumor Agents* (Borders, D. B., and Doyle, T. W., Eds.) pp 1–15, Marcel Dekker, New York.
- Dedon, P. C., and Goldberg, I. H. (1992) Free-radical mechanisms involved in the formation of sequence-dependent bistranded DNA lesions by the antitumor antibiotics bleomycin, neocarzinostatin, and calicheamicin. *Chem. Res. Toxicol.* **5**, 311–332.
- Zein, N., Poncin, M., Nilakantan, R., and Ellestad, G. A. (1989) Calicheamicin  $\gamma_1^I$  and DNA: molecular recognition process responsible for site-specificity. *Science* **244**, 697–699.
- Walker, S., Landovitz, R., Ding, W. D., Ellestad, G. E., and Kahne, D. (1992) Cleavage behavior of calicheamicin  $\gamma_1^I$  and calicheamicin T. *Proc. Natl. Acad. Sci. U.S.A.* **89**, 4608–4612.
- Zein, N., Ding, W.-D., and Ellestad, G. A. (1990) Interaction of calicheamicin with DNA, in *Molecular Basis of Specificity in Nucleic Acid-Drug Interactions* (Jortner, B. P. a. J., Ed.) pp 323–330, Kluwer Academic Publishers, Dordrecht, The Netherlands.
- Yu, L., Salzberg, A. A., and Dedon, P. C. (1995) New insights into calicheamicin–DNA interactions derived from a model nucleosome system. *Bioorg. Med. Chem.* **3**, 729–741.
- Mah, S. C., Price, M. A., Townsend, C. A., and Tullius, T. D. (1994) Features of DNA recognition for oriented binding and cleavage by calicheamicin. *Tetrahedron* **50**, 1361–1378.
- Walker, S., Murnick, J., and Kahne, D. J. (1993) Structural characterization of a calicheamicin–DNA complex by NMR. *J. Am. Chem. Soc.* **115**, 7954–7961.
- Walker, S. L., Andreotti, A. H., and Kahne, D. E. (1994) NMR characterization of calicheamicin  $\gamma_1^I$  bound to DNA. *Tetrahedron* **50**, 1351–1360.
- Paloma, L. G., Smith, J. A., Chazin, W. J., and Nicolaou, K. C. (1994) Interaction of calicheamicin with duplex DNA: Role of the oligosaccharide domain and identification of multiple binding modes. *J. Am. Chem. Soc.* **116**, 3697–3708.
- Kumar, R. A., Ikemoto, N., and Patel, D. J. (1997) Solution structure of the calicheamicin  $\gamma_1^I$ –DNA complex. *J. Mol. Biol.* **265**, 187–201.
- Ikemoto, N., Kumar, R. A., Ling, T.-T., Ellestad, G. A., Danishefsky, S. J., and Patel, D. J. (1995) Calicheamicin–DNA complexes: Warhead alignment and saccharide recognition of the minor groove. *Proc. Natl. Acad. Sci. U.S.A.* **92**, 10506–10510.
- Krishnamurthy, G., Brenowitz, M. D., and Ellestad, G. A. (1995) Salt dependence of calicheamicin–DNA site-specific interactions. *Biochemistry* **34**, 1001–10.
- Drak, J., Iwasawa, N., Danishefsky, S., and Crothers, D. M. (1991) The carbohydrate domain of calicheamicin  $\gamma_1^I$  determines its sequence specificity for DNA cleavage. *Proc. Natl. Acad. Sci. U.S.A.* **88**, 7464–7468.
- Aiyar, J., Danishefsky, S. J., and Crothers, D. M. (1992) Interaction of the aryl tetrasaccharide domain of calicheamicin  $\gamma_1^I$  with DNA: Influence of aglycon and methidiumpropyl–EDTA–iron(II)-mediated DNA cleavage. *J. Am. Chem. Soc.* **114**, 7552–7554.
- Ding, W.-d., and Ellestad, G. A. (1991) Evidence for a hydrophobic interaction between calicheamicin and DNA. *J. Am. Chem. Soc.* **113**, 6617–6620.
- Rentzeperis, D., Kupke, D., and Marky, L. (1992) Differential hydration of homopurine sequences relative to alternating purine/pyrimidine sequences. *Biopolymers* **32**, 1065–1075.
- Kuduvalli, P. N., Townsend, C. A., and Tullius, T. D. (1995) Cleavage by calicheamicin  $\gamma_1^I$  of DNA in a nucleosome formed on the 5S RNA gene of *Xenopus borealis*. *Biochemistry* **34**, 3899–3906.
- Sissi, C., Aiyar, J., Boyer, S., Depew, K., Danishefsky, S., and Crothers, D. M. (1999) Interaction of calicheamicin  $\gamma_1^I$  and its related carbohydrates with DNA–protein complexes. *Proc. Natl. Acad. Sci. U.S.A.* **96**, 10643–10648.
- Krishnamurthy, G., Ding, W.-d., O'Brien, L., and Ellestad, G. A. (1994) Circular dichroism studies of calicheamicin–DNA interactions: Evidence for a calicheamicin-induced DNA conformational change. *Tetrahedron* **50**, 1341–1349.
- LaMarr, W. A., Nicolaou, K. C., and Dedon, P. C. (1998) Supercoiling affects the accessibility of glutathione to DNA-bound molecules: Positive supercoiling inhibits calicheamicin-induced DNA damage. *Proc. Natl. Acad. Sci. U.S.A.* **95**, 102–107.
- Salzberg, A. A., and Dedon, P. C. (1997) An improved method for the rapid assessment of DNA bending by small molecules. *J. Biomol. Struct. Dyn.* **15**, 277–284.

30. Ausubel, F. M., Brent, R., Kingston, R. E., Moore, D. D., Seidman, J. G., Smith, J. A., and Struhl, K. (1989) *Current Protocols in Molecular Biology*, John Wiley and Sons, New York.
31. Bolshoy, A., McNamara, P., Harrington, R. E., and Trifonov, E. N. (1991) Curved DNA without A-A: experimental estimation of all 16 DNA wedge angles, *Proc. Natl. Acad. Sci. U.S.A.* 88, 2312–2316.
32. McNamara, P. T., and Harrington, R. E. (1991) Characterization of inherent curvature in DNA lacking polyadenine runs, *J. Biol. Chem.* 266, 12548–12554.
33. Ulanovsky, L., Bodner, M., Trifonov, E. N., and Choder, M. (1986) Curved DNA: Design, synthesis, and circularization, *Proc. Natl. Acad. Sci. U.S.A.* 83, 862–866.
34. Taylor, W. H., and Hagerman, P. J. (1990) Application of the method of phage T4 DNA ligase-catalyzed ring-closure to the study of DNA structure. II. NaCl-dependence of DNA flexibility and helical repeat, *J. Mol. Biol.* 212, 363–376.
35. Crothers, D., Drak, J., Kahn, J., and Levene, S. (1992) DNA bending, flexibility, and helical repeat by cyclization kinetics, *Methods Enzymol.* 212, 3–30.
36. Kahn, J. D., and Crothers, D. M. (1992) Protein-induced bending and DNA cyclization, *Proc. Natl. Acad. Sci. U.S.A.* 89, 6343–6347.
37. Mah, S. C., Townsend, C. A., and Tullius, T. D. (1994) Hydroxyl radical footprinting of calicheamicin. Relationship of DNA binding to cleavage, *Biochemistry* 33, 614–621.
38. Nicolaou, K. C., Li, T., Nakada, M., Hummel, C. W., Hiatt, A., and Wrasildo, W. (1994) Calicheamicin  $\phi_1$ : A rationally designed molecule with extremely potent and selective DNA cleaving properties and apoptosis inducing activity, *Angew. Chem., Int. Ed. Engl.* 33, 183–186.
39. Crothers, D. M., Haran, T. E., and Nadeau, J. G. (1990) Intrinsically Bent DNA, *J. Biol. Chem.* 265, 7093–7096.
40. Diekmann, S. (1992) Analyzing DNA curvature on polyacrylamide gels, *Methods Enzymol.* 212, 30–46.
41. Hagerman, P. J. (1990) Sequence-directed curvature of DNA, *Annu. Rev. Biochem.* 59, 755–781.
42. Kahn, J. D., Yun, E., and Crothers, D. M. (1994) Detection of localized DNA flexibility, *Nature* 368, 163–166.
43. Shore, D., Langowski, J., and Baldwin, R. L. (1981) DNA flexibility studied by covalent closure of short fragments into circles, *Proc. Natl. Acad. Sci. U.S.A.* 78, 4833–4837.
44. Hagerman, P. J., and Ramadevi, V. A. (1990) Application of the method of phage T4 ligase-catalyzed ring-closure to the study of DNA structure. I. Computational analysis, *J. Mol. Biol.* 212, 351–362.
45. Shore, D., and Baldwin, R. L. (1983) Energetics of DNA twisting. II. Topoisomer analysis, *J. Mol. Biol.* 170, 983–1007.
46. Koo, H.-S., Drak, J., Rice, J. A., and Crothers, D. M. (1990) Determination of the extent of DNA bending by an adenine–thymine tract, *Biochemistry* 29, 4227–4234.
47. Chatterjee, M., Mah, S. C., Tullius, T. D., and Townsend, C. A. (1995) Role of the aryl iodide in the sequence-selective cleavage of DNA by calicheamicin. Importance of thermodynamic binding vs kinetic activation in the cleavage process, *J. Am. Chem. Soc.* 117, 8074–8082.
48. Nicolaou, K. C., Smith, A. L., and Yue, E. W. (1993) Chemistry and biology of natural and designed enediynes, *Proc. Natl. Acad. Sci. U.S.A.* 90, 5881–5888.
49. Wu, J., Xu, J., and Dedon, P. C. (1999) Modulation of enediyne-induced DNA damage by chromatin structures in transcriptionally active genes, *Biochemistry* 38, 15641–6.
50. Walker, S., Valentine, K. G., and Kahne, D. J. (1990) Sugars as DNA binders — A comment on the calicheamicin oligosaccharide, *J. Am. Chem. Soc.* 112, 6428–6429.
51. Bruckner, I., Dlakic, M., Savic, A., Susic, S., Pongor, S., and Suk, D. (1993) Evidence for opposite groove-directed curvature of GGGCCC and AAAAAA sequence elements, *Nucleic Acids Res.* 21, 1025–1029.
52. Koo, H.-S., Wu, H.-M., and Crothers, D. M. (1986) DNA bending at adenine–thymine tracts, *Nature* 320, 501–506.

BI992227G